JOURNAL OF GEOPHYSICAL RESEARCH, VOL. 102, NO. B3, PAGES 5231–5242, MARCH 10, 1997

Numerical simulation of high-pressure rock tensile fracture experiments: Evidence of an increase in fracture energy with pressure?

Yuri A. Fialko and Allan M. Rubin

Department of Geosciences, Princeton University, Princeton, New Jersey

Abstract. High confining pressure fracture tests of Indiana limestone [*Abou-Sayed*, 1977] and Iidate granite [*Hashida et al.*, 1993] were simulated using boundary element techniques and a Dugdale-Barenblatt (tension-softening) model of the fracture process zone. Our results suggest a substantial (more than a factor of 2) increase in the fracture energy of Indiana limestone when the confining pressure was increased from zero to only 6-7 MPa. While *Hashida et al.* [1993] concluded that there was no change in the fracture energy of Iidate granite at confining pressures up to 26.5 MPa, we find that data from one series of experiments ("compact-tension" tests in their terminology) are also consistent with a significant (more than a factor of 2) increase in fracture energy. Data from another set of their experiments (thick-walled cylinder tests) seem to indicate a decrease in the fracture energy of Iidate granite at confining pressures of 6-8 MPa, but these may be biased due to the very small specimen size. To our knowledge these results are the first reliable indication from laboratory experiments that rock tensile fracture energy varies with confining pressure. Based on these results, some possible mechanisms of pressure sensitive fracture are discussed. We suggest that the inferred increase in fracture energy results from more extensive inelastic deformation near the crack tip that increases the effective critical crack opening displacement. Such deformation might have occurred due to the large deviatoric stress in the vicinity of the crack tip in the Abou-Sayed experiments, and due to the enlarged region of significant tensile stress near the crack tip in the Hashida et al. compact tension tests. These results also highlight the fact that at confining pressures that exceed the tensile strength of the material, tensile fracture energy will in general depend upon the crack size and the distribution of loads within it, as well as the ambient stress.

Introduction

Existing theoretical models of fluid-driven crack propagation in the Earth commonly assume that the rock fracture energy is insignificant compared to the energy associated with viscous dissipation in the fluid [*Stevenson*, 1982; *Spence and Turcotte*, 1985; *Lister and Kerr*, 1991]. This assumption results from the application of linear elastic fracture mechanics (LEFM) to the description of a fluid fracture at depth. In LEFM, the resistance of rock to tensile fracture is assumed to be a material property governed by a single parameter which may be taken to be either the fracture toughness K_{1c} or the fracture energy G_{1c}. The fracture toughness, with units of Pa $m^{1/2}$, is a measure of the strength of the (theoretical) stress singularity at the crack tip required for crack propagation, and the fracture energy, with units of J m^{-2}, is the energy (per unit area) required to fracture a material. Provided that the values of K_{1c} or G_{1c} measured at atmospheric pressure are applicable under in situ conditions, fracture resistance becomes negligible when the crack length exceeds some nominal value (of the order of meters for excess fluid pressures of a few megapascals [see, e.g., *Lister and Kerr*, 1991]).

Copyright 1997 by the American Geophysical Union.

Paper number 96JB03859.
0148-0227/97/96JB-03859$09.00

While K_{1c} and G_{1c} may be considered to be equivalent when LEFM is applicable [e.g., *Lawn and Wilshaw*, 1975], K_{1c} is the parameter that is more commonly encountered in the geological literature and is the parameter that has been reported in most high-pressure rock tensile fracture experiments [*Atkinson and Meredith*, 1987; *Thiercelin*, 1987; *Roegiers and Zhao*, 1991]. However, it has recently been shown that at confining pressures that exceed the tensile failure strength of the material, there is no one-to-one correspondence of fracture toughness and fracture energy, and "fracture toughness" is ill defined [*Rubin*, 1993; *Hashida et al.*, 1993; *Khazan and Fialko*, 1995]. In essence, this is because at high confining pressure the elastic stress field surrounding the crack tip process zone (the region where fracture of the intact material takes place) is not well approximated by a square root stress singularity, which violates a basic assumption underlying LEFM. One consequence of this is that the "apparent" fracture toughness may increase with confining pressure, and vary with different loading configurations at the same confining pressure, even if the fracture energy is independent of loading configuration and confining pressure. In addition, the experimentally determined "apparent" toughness depends in an essential way upon the inferred position of the crack tip within the specimen. The crack tip is assumed to be mathematically sharp for purposes of interpreting the experimental data [e.g., *Schmidt and Huddle*, 1977], but the size of the process zone

cannot be neglected when the confining pressure exceeds the failure stresses within the process zone [*Rubin*, 1993]. For these reasons, most reports of variations in fracture toughness with confining pressure cannot be interpreted as reflecting variations in rock fracture properties.

As an alternative to the LEFM approach, a more physical Barenblatt-type model of the crack tip [*Barenblatt*, 1962] has been proposed for geophysical applications [e.g. *Ingraffea*, 1987]. The Barenblatt model, also referred to as a Dugdale-Barenblatt (DB) model, assumes that fracture is resisted by cohesive stresses σ_T acting across a thin process zone ahead of the crack tip; nonelastic deformation is thus restricted to the crack plane and fracture is defined to be complete when a critical crack wall separation δ_c is exceeded. Experimental data confirm that process zones in rocks are typically only a few grains across and elongate in the plane of the fracture [*Swanson*, 1987; *Labuz et al.*, 1987]. The dependence of cohesive stresses σ_T on crack opening δ is called the tension-softening relation. The fracture energy G_c in the case of a DB model is the work required to separate the two crack faces, or, equivalently, the area under the tension-softening curve (see, for example, Figure 3):

$$G_c = \int_0^{\delta_c} \sigma_T(\delta)\, d\delta \ . \qquad (1)$$

Because fluid-driven crack propagation at depth results in absolute tension at the crack tip, it is possible that the details of failure within the process zone are independent of the confining pressure, and that the tension-softening relation (and hence the fracture energy) is an intrinsic rock property. *Hashida et al.* [1993] performed several series of fracture tests of Iidate granite at confining pressures from 0 to 26.5 MPa and concluded that over this pressure range the tension-softening behavior of the granite is independent of pressure.

At the same time, industrial hydraulic fracture treatments [*Cleary et al.*, 1991; *Shlyapobersky and Chudnovsky*, 1992] as well as field studies of eroded dikes [*Delaney et al.*, 1986] indicate that in situ values of fracture energy appear to be considerably larger than those inferred from zero pressure laboratory tests. Several models have been proposed to explain this discrepancy. One explanation holds that laboratory-scale specimens do not sample the large-scale defects which are present in rock massifs. Since larger cracks may interact with larger defects, the process zone size (and the fracture energy) may scale with crack length [*Dyskin and Germanovich*, 1993]. In addition, *Rubin* [1993] demonstrated that larger-than-lab process zones may result from the stress perturbation surrounding the low-pressure region ahead of the fluid front within propagating cracks at depth. However, the effects of confining pressure and loading configuration (e.g., crack size, crack pressure, ambient deviatoric stress, etc.) on key fracture parameters of rocks (such as tensile strengths σ_T, critical opening displacements δ_c, and fracture energies G_c) remain poorly understood.

In the present study we use a numerical technique similar to that employed by *Hashida et al.* [1993] to investigate the pressure dependence of rock fracture properties, using previously reported data from high-pressure tensile fracture experiments (hereinafter, by "high pressure" we imply pressures that exceed the peak tensile strength of a material). Our simulation of thick-walled cylinder tests of Indiana limestone [*Abou-Sayed*, 1977] suggests an increase in fracture energy of more than a factor of 2 as the confining pressure is raised from 0 to 7 MPa . We also show that the high-pressure experiments of *Hashida et al.* [1993] do not suggest pressure independence of the fracture energy of Iidate granite; in fact, the results of their compact tension tests seem to reflect an increase in fracture energy by a factor of 2 or more at 26.5 MPa confining pressure. On the other hand, their thick-walled cylinder experiments may indicate a substantial decrease in the fracture energy at confining pressures of 6 to 8 MPa. These experiments are, to the best of our knowledge, the only high-pressure experiments that can be simulated using a DB model. As pointed out by *Hashida et al.* [1993], in general, such modeling requires complete load-displacement records, which have not been reported for most stable fracture experiments [e.g., *Schmidt and Huddle*, 1977; *Thiercelin*, 1987]. Thick-walled cylinder experiments represent an exception, in that load-displacement records are useful but not essential since the breakdown pressure is an unambiguous data point that one can attempt to reproduce numerically.

It should be emphasized that even if the experiments discussed below could be interpreted unambiguously, they are insufficient to reach completely general conclusions regarding rock fracture energy at depth. A final consequence of the breakdown of LEFM at high confining pressure is that the stress field surrounding the tip of a stably propagating crack depends upon the particular crack (its size and internal load distribution) as well as the confining pressure (or, more appropriately, the ambient stress) [*Rubin*, 1993]. Therefore fracture energy at high confining pressure should not be considered to be a material property, and the full range of possible fracture behaviors cannot be characterized from a small number of experiments. Nonetheless, if the causes of fracture energy variation for high confining pressure experiments can be understood, it may be possible to extrapolate these results and predict fracture energy variations for particular cases of interest in the Earth. The possibility of significant increases of fracture energy with depth and crack size, suggested by the field and hydrofracture observations, provides the incentive for this study.

Experimental Setting and Numerical Results

Simulations of Thick-Walled Cylinder Experiments for Limestone

Abou-Sayed [1977] implemented several series of thick-walled cylinder (TWC) tests of Indiana limestone at confining pressures up to 6.9 MPa. All samples were precut with two radially symmetric notches placed along the inner hole to the depth of one-tenth of the cylinder wall. Both at atmospheric and high confining pressures the specimen was loaded by increasing the internal pressure until the sample burst; in the high pressure tests the external (confining) pressure P_c was increased simultaneously with the internal pressure P_i in the ratio $P_c/P_i = 0.125$. The sample dimensions, applied loads and results of these experiments are summarized in Table 1.

Modified versions of the constant [*Crouch and Starfield*, 1983] and quadratic [*Brebbia and Dominguez*, 1991] boundary element codes for two-dimensional elastostatic problems were employed in our analysis. The techniques gave essentially the

Table 1. Experimental Data of *Abou-Sayed* [1977] TWC Tests

Test	Internal Diameter, mm	External Diameter, mm	Height, mm	Axial Stress, MPa	Confining pressure, MPa	Internal Pressure, MPa
1	9.5	104	47	0.7	0	18.1
2	9.5	104	46	0.7	0	16.0
3	9.5	104	43	0.7	0	15.5
4	9.5	104	104	0.7	0	16.7
5	9.5	104	104	0.7	0	14.7
13	9.5	64	64	6.0	6.0	48.0
14	9.5	64	64	6.9	6.9	54.8
15	9.5	64	64	6.3	6.3	50.1

same results. Crack and process zone growth were simulated using an iterative procedure. At the start of each iteration, the known boundary conditions were satisfied along the entire boundary of the specimen; the resulting stresses and displacements along the prospective crack growth line were then analyzed and the boundary conditions on this line were modified in accordance with the tension-softening relation. Process zone growth was taken to occur if the normal stress across a node ahead of the crack tip exceeded the tensile strength σ_T. If the opening at a node along the crack line exceeded the critical value δ_c, the stresses at this node were dropped to zero and it became part of the "developed" (stress-free) crack. Iterations were continued until stresses along the crack growth line converged to an equilibrium solution with an accuracy of 0.1%. Figure 1 shows the boundary element mesh used for the high-pressure configuration. Following an initial phase of stable crack growth as the load is increased, unstable growth is apparent when the opening at all nodes along the prospective crack path becomes supercritical and no equilibrium solution is obtained.

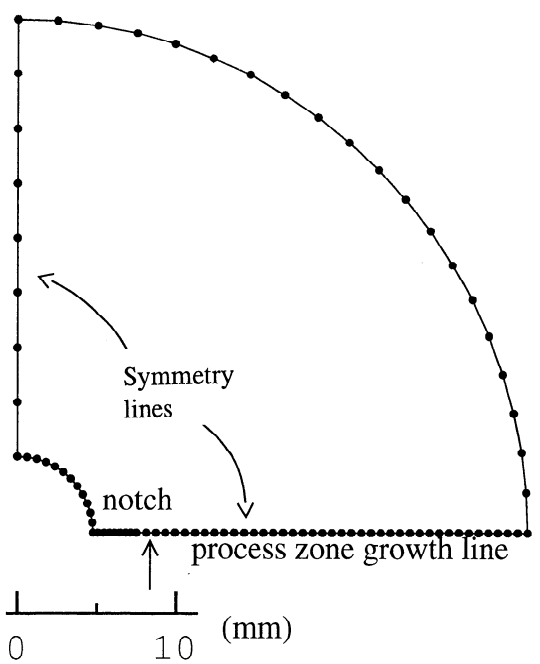

Figure 1. Boundary element mesh used in simulation of thick-walled cylinder (TWC) tests of *Abou-Sayed* [1977].

Although a zero-pressure tension-softening relation for Indiana limestone is not available, our simulations show that for reasonable values of the peak tensile strength (which is more or less constrained by the bulk tensile strength determined in direct pull tests [*Ingraffea*, 1987; *Hashida et al.*, 1993]), the theoretical breakdown pressure depends upon the fracture energy and not on details of the tension-softening relation (Figure 2). In LEFM this dependence of the critical load upon fracture energy alone is expected provided that the process zone is a small fraction of the crack length [*Rice*, 1968]. It appears that for the TWC configuration the requirement of the process zone dimension is even less strict; in this case dependence of the breakdown (burst) pressure upon the fracture energy alone requires only that the crack wall separation exceeds δ_c at the base of the process zone before catastrophic rupture (i.e., that the length of the full-size equilibrium process zone be less than the specimen thickness).

For a peak tensile strength of 4-6 MPa [*Schmidt*, 1976; *Weinberger et al.*, 1994], atmospheric pressure values of the fracture energy of 10-30 J m^{-2} are inferred for Indiana

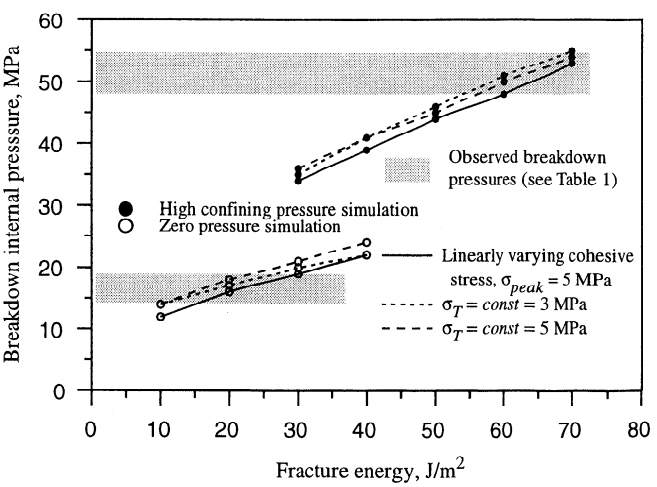

Figure 2. Predicted dependence of the breakdown pressure on the fracture energy of Indiana limestone in the TWC experiments of *Abou-Sayed* [1977]. Critical opening displacement δ_c equals G_c/σ_T for a constant cohesive stress model, and δ_c equals $2G_c/\sigma_T$ for a linearly varying cohesive stress model. Shaded areas show the limits of the observed breakdown pressures in zero and high confining pressure tests.

limestone (note from Figure 2 that small variations in the internal breakdown pressure imply large variations in the fracture energy). Within the sensitivity of the experiments, these values are consistent with zero-pressure values obtained using the standard LEFM relation between the fracture energy and fracture toughness $G_c = K_{1c}^2(1-\nu^2)/E$, where E is Young's modulus and ν is Poisson's ratio. For Indiana limestone, $K_{1c} \sim 1$ MPa m$^{1/2}$, $E \sim 32$ GPa and $\nu \sim 0.21$ [*Schmidt*, 1976], yielding $G_c \sim 30$ J m^{-2}. In contrast, the observed breakdown pressures in the high confining pressure experiments can be matched only with a fracture energy of 60-70 J m^{-2} (Figure 2). Note that for any particular fracture energy an increase in σ_T to values greater than those assumed would reduce the size of the process zone and lead to curves essentially coincident with those shown. A significant reduction in σ_T would lead to curves falling below those shown. In the latter case it is possible to satisfy both the zero and high confining pressure data with a fracture energy of 60-70 J m^{-2}. However, this would require unrealistically low values of the tensile strength (2 MPa or less) and would also be inconsistent with independent zero-pressure estimates of G_c. Since the numerical calculations show that the breakdown pressures in the experiments of *Abou-Sayed* [1977] depend alone on the fracture energy for any value of tensile strength in excess of ~ 3 MPa, the inferred increase in the fracture energy of Indiana limestone in these experiments seems to be robust.

Simulations of Compact Tension and Thick-Walled Cylinder Experiments for Granite

Hashida et al. [1993] performed a set of fracture tests on Iidate granite using a compact tension (CT) configuration (at confining pressures ranging from 0 to 26.5 MPa) and a TWC configuration (at confining pressures from 0 to 8 MPa). Load-displacement curves were recorded in the CT tests; TWC specimens were loaded to failure by increasing the fluid pressure in the inner hole of the cylinders (which were not pre-notched) while the external (confining) pressure was kept fixed (see *Hashida et al.* [1993] for details). The data obtained were compared to the results of a boundary element model that simulated the tension-softening behavior of Iidate granite determined independently at atmospheric pressure (Figure 3). The calculated and experimental data revealed a satisfactory match at both zero and high confining pressure, leading the authors to conclude that the tension-softening relation of Iidate granite is independent of confining pressure. Because our simulation of the Abou-Sayed experiments led to the opposite conclusion, we implemented a numerical test of the sensitivity of the experiments of *Hashida et al.* [1993] to variations in the tension-softening behavior.

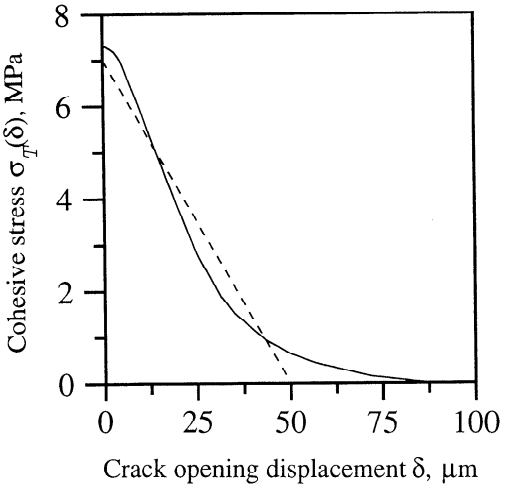

Figure 3. Tension-softening relations used in the boundary element simulations of *Hashida et al.* [1993] experiments. Solid line, measured tension-softening curve for Iidate granite [*Hashida et al.*, 1993]; dashed line, linearly varying cohesive stress model. Area bounded by each curve equals the fracture energy G_c (~ 175 J m^{-2}). Several simulations demonstrated that a linear approximation to the measured tension-softening curve, chosen such that the values of fracture energy and peak strength remain the same, give results that are practically indistinguishable from those obtained using the measured tension-softening relation.

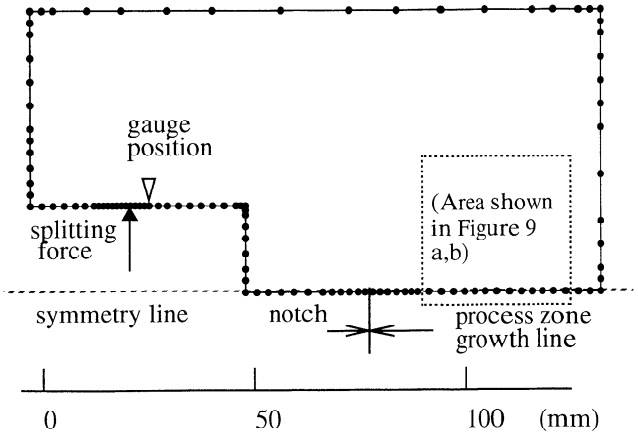

Figure 4. Boundary element mesh used in the simulation of compact tension (CT) tests of *Hashida et al.* [1993]. The vertical scale is the same as the horizontal one.

The boundary element mesh used in the simulation of the CT tests of *Hashida et al.* [1993] is shown in Figure 4. A displacement boundary condition was prescribed on the boundary element corresponding to the point at which the splitting load was applied in the actual experiments. The resulting normal stress across this element was used to infer the value of the applied load per unit thickness, and the specimen displacement Δ was obtained by doubling (because of symmetry) the normal displacement of the node corresponding to the gauge position (see Figure 4). Confining pressure was applied along the rest of the specimen boundary except the symmetry line, which consists of a precut notch (isolated from the pressurizing fluid) and the line of prospective crack growth. Along the precut notch both normal and shear tractions were set to zero. Along the prospective crack growth line the shear stress was set to zero, the normal displacement was set to zero ahead of the crack tip, and once the peak strength at a node was exceeded, the normal stress was constrained (by iteration) to be consistent with the resulting normal displacement according to the tension-softening relation. The results of our simulation are shown along with the experimental data in Figure 5. Our predicted load-displacement curves calculated using a linear approximation to the zero-pressure tension-softening relation (short-dashed lines in Figure 5) are nearly identical to those computed by *Hashida et al.* [1993] using the "actual" zero-pressure tension-softening relation (see Figure 3). This

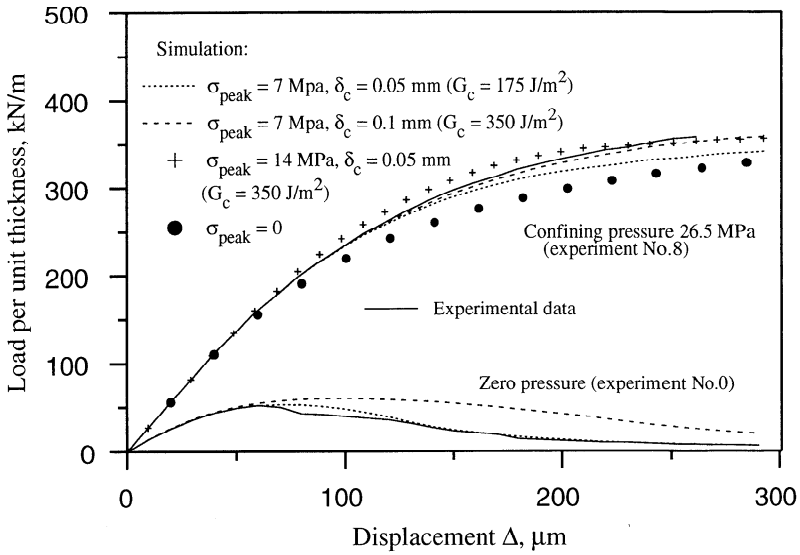

Figure 5. Experimental and calculated load-displacement curves for CT tests of *Hashida et al.* [1993] at zero and 26.5 MPa confining pressures. Experimental data are taken from Figure 10 of *Hashida et al.* [1993]. Short-dashed lines represent the results of the simulation using the linear approximation to the "true" zero-pressure tension-softening curve (Figure 3). Long-dashed lines correspond to the linearly varying cohesive stress model with a doubled value of δ_c (and hence G_c). High-pressure experimental curve is even better approximated assuming a threefold increase in δ_c. Pluses correspond to a twofold increase in the peak cohesive stress and zero-pressure value of δ_c. Solid circles show the computed load-displacement curve assuming no cohesion along the symmetry line. The origin of the plot is taken to correspond to the displacement and load when the base of the precut notch has zero normal displacement.

demonstrates that minor differences in the tension-softening law have little impact on the numerical results provided that the fracture energy is the same.

As is seen from Figure 5, the results of our simulations for different values of the fracture parameters reveal a critical opening displacement, and hence fracture energy, for the high confining pressure experiment that is greater than that at zero pressure by a factor of 2 or more. While a factor of 2 increase in critical opening displacement (long-dashed curve) provides a fit that is very close to the experimental data (solid curve), a factor of 3 increase actually gives rise to a load-displacement curve that is indistinguishable from the data. The experimental configuration is not very sensitive to increases in excess of a factor of 2 because in such cases δ_c is not reached along the crack line for the displacement range covered by the experiment. Modeling of the other 26.5 MPa tests of *Hashida et al.* [1993, Figure 11] also suggests a factor of 2 or more increase in δ_c.

The sensitivity of the experimental results to increases in the fracture energy due to increases in δ_c is much less at high confining pressure than at atmospheric pressure (Figure 5). This may be explained by the fact that at high pressure most of the work done in breaking the specimen is spent against the confining pressure (26 MPa) rather than the cohesive stresses (7 MPa); this may also be seen from the crudely similar appearance of all the high-pressure curves to that computed assuming a cohesive stress of zero (solid circles). The general similarity of the experimental data to the curve computed using zero-pressure fracture parameters may account for the acceptance by Hashida et al. of those parameters when fitting the high-pressure data. Note that the fit to the experimental data is degraded if the twofold increase in fracture energy is assumed to result from an increase in the cohesive stress (pluses in Figure 5). Qualitatively, increases in σ_T extend the initially linear portion of the load-displacement curves to larger displacements, while increases in δ_c prevent the curves from flattening out (maintain "work-hardening" behavior) at larger displacements.

In the TWC tests of *Hashida et al.* [1993] the internal and external pressures were applied simultaneously to a predetermined level, and then the internal pressure was increased until catastrophic failure of the specimen occurred. The boundary element mesh approximating the TWC geometry is shown in Figure 6, and experimental and simulation data are shown in Figure 7. Increases in δ_c affect the predicted breakdown pressure only slightly (Figure 7). The primary

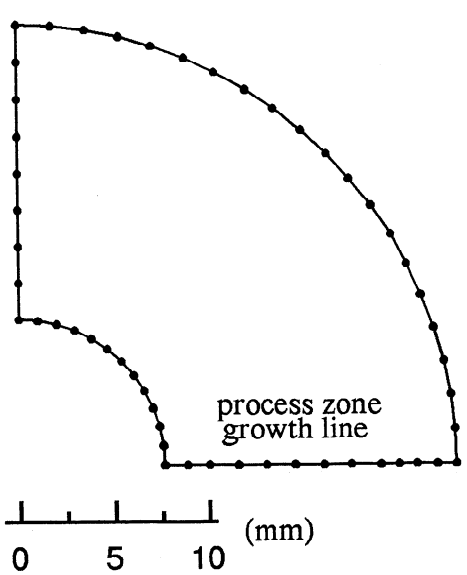

Figure 6. Boundary element mesh, used in the simulation of TWC tests of *Hashida et al.* [1993]. Radial lines are symmetry planes.

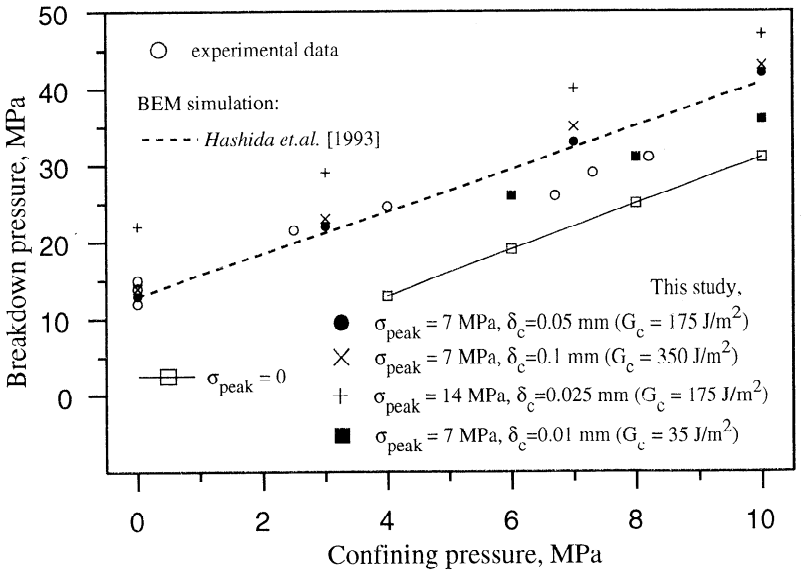

Figure 7. Observed and predicted values of the breakdown pressure for TWC tests of *Hashida et al.* [1993]. Experimental data (open circles) and calculated breakdown pressures corresponding to the "true" tension softening relation (dashed line) are taken from *Hashida et al.* [1993, Figure 16]. Linear gradient cohesive stress models for both atmospheric pressure values of δ_c (solid circles) and doubled atmospheric pressure values of δ_c (crosses) produce results which are close to those obtained using the "true" zero-pressure tension-softening relation. On the other hand, a twofold increase in the peak tensile strength (pluses) gives rise to breakdown pressures which are markedly different from the observed values, even if δ_c is reduced so that the fracture energy is unchanged. At confining pressures from 6 to 8 MPa, the observed breakdown pressures are best matched with a twofold decrease in the peak cohesive strength (not shown) or a factor of 5 decrease in δ_c (solid squares).

reason for the insensitivity of the breakdown pressure to δ_c in this case is not the confining pressure, which was only of the order of the cohesive strength, but the small specimen size. Examination of the last stable boundary element solution (prior to burst) indicates that, in the range of confining pressures tested, failure of the TWC specimens always takes place before the zero-pressure (or larger) δ_c is reached anywhere within the process zone. Under such conditions failure is controlled by the tensile strength to a greater extent than by the fracture energy of the material (e.g., compare the breakdown pressures predicted for the twofold increase in the cohesive stress (pluses in Figure 7) and the twofold increase in the critical opening (crosses in Figure 7) to the breakdown pressures calculated assuming zero-pressure values of σ_T and δ_c (filled circles)). The thickness of the cylinder wall used by *Hashida et al.* [1993] was only 15 mm, whereas an equilibrium process zone length for Iidate granite at 6 MPa confining pressure is estimated to be of the order of 100 mm (Appendix A). In the high confining pressure configuration of Abou-Sayed, there was always a phase of stable propagation where the crack wall separation exceeded δ_c, because of the smaller cohesive zone and the larger specimen size.

Taken at face value, the results of the TWC tests of Hashida et al. show little change in the fracture energy of Iidate granite at confining pressures less than 4 MPa, but a substantial decrease in the fracture energy at confining pressures of 6-8 MPa (Figure 7). Fitting of the experimental data shows that the low breakdown pressures at elevated confining pressures may be explained by a factor of 2 drop in the peak tensile strength or a factor of five decrease in the critical opening displacement, relative to those parameters at zero pressure (solid squares in Figure 7). If correct, then there is an apparent discrepancy between the inferred trends of fracture energy in the high-pressure CT and TWC tests of Iidate granite and also a discrepancy between the TWC tests of Iidate granite and Indiana limestone. Possible reasons for this discrepancy are considered in the discussion below. On the other hand, if the low breakdown pressures in the 6 - 8 MPa Iidate granite TWC tests are due only to experimental scatter (a view apparently adopted by Hashida et al.), then both series of granite experiments are consistent with an increase in the critical opening displacement of a factor of 2 or more. In addition, both series of experiments show that the tensile strength of Iidate granite does not increase significantly with confining pressure, provided that the critical opening displacement does not decrease even more dramatically with confining pressure. This conclusion stems from the fact that a significant increase in the cohesive stress would be detected from the data (see pluses in Figures 5 and 7).

Discussion

Several possible explanations for the inferred increase of fracture energy of Indiana limestone in the TWC tests of *Abou-Sayed* [1977] were explored. First, the stress field in the specimen was examined to see if it was consistent with the assumption that inelastic deformation was restricted to the crack plane. Figure 8 shows the minimum (σ_1) and maximum (σ_2) compressive stresses at the last stable loading condition at zero and high confining pressures, using a constant cohesive stress model of the process zone. The region around the process zone subjected to tensile stresses near the tensile strength is smaller at high pressure than at atmospheric pressure (e.g., compare the areas bounded by the $0.8\,\sigma_T$ contour lines in Figures 8a and 8c; note the scale difference between the two figures). Thus more extensive tensile

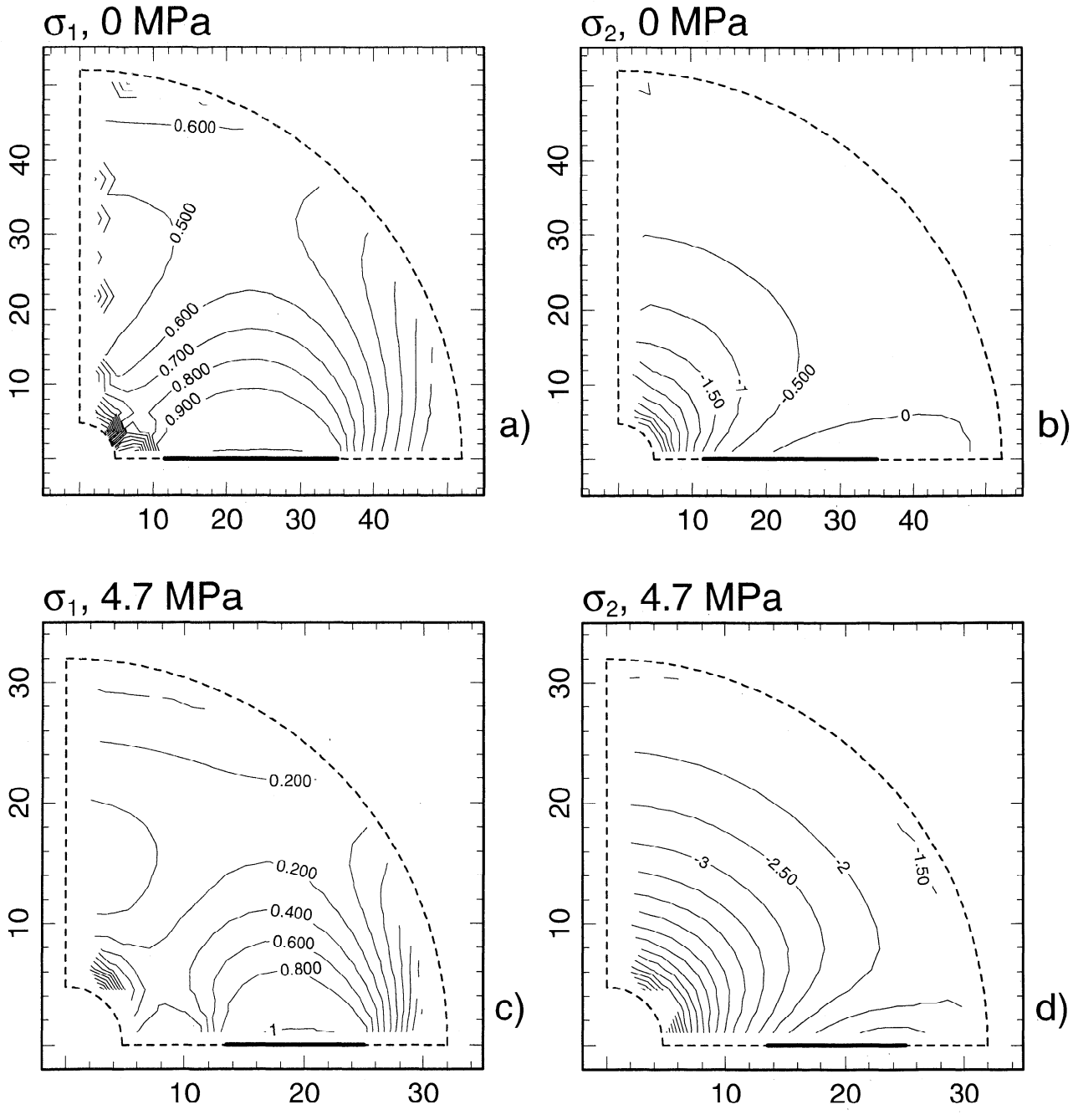

Figure 8. (a, c) The minimum and (b, d) the maximum compressive stresses upon final stable loading for (a, b) zero-pressure and (c, d) high confining pressure TWC configurations of *Abou-Sayed* [1977] for σ_T = const = 3 MPa and δ_c = 0.01 mm (G_c = 30 J m^{-2}). All stresses are normalized by the tensile strength (3 MPa). Bold solid lines show the position of the process zone. Dashed lines show the sample boundary and symmetry axes. Stresses cannot be resolved close to the specimen boundary because of the singular character of stresses at the boundary element nodes.

cracking may not be the explanation for the apparent increase in fracture energy at high confining pressure. However, Figure 8 shows that considerably larger stress anisotropy occurs at high confining pressure than at zero pressure, and that stress conditions close to pure shear exist over some region off the crack plane in the high-pressure configuration. Although the maximum compressive stresses are not large enough to induce macroscopic shear fractures, the material in the near-tip region is subjected to stresses that are closer to a shear failure envelope (e.g., the Navier-Coulomb envelope) at high confining pressure than at zero pressure. Given that the onset of microcracking in compression tests starts well below the peak failure stress, particularly for porous rocks [*Lockner et al.*, 1992], it seems possible that some inelastic strain can accumulate off of the crack plane.

Figure 8 also shows that the tensile strength is exceeded in the vicinity of the inner hole of the cylinder. To account for the effect of possible fracture damage in this region, tension-softening was allowed to occur along several radial lines of boundary elements in addition to the "main" crack growth

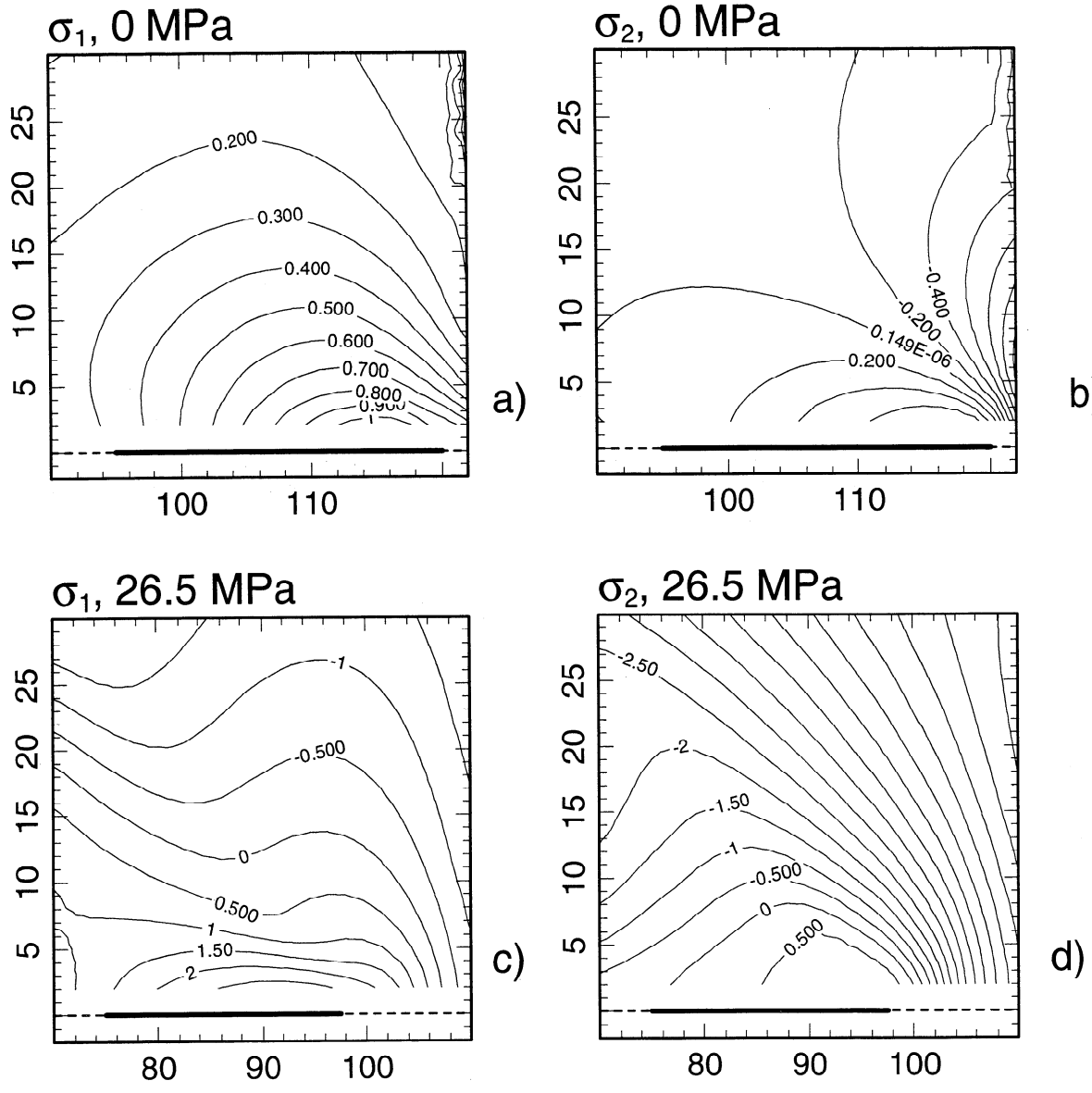

Figure 9. (a, c) The minimum and (b, d) the maximum compressive stresses in the vicinity of the process zone for (a, b) zero-pressure and (c, d) high confining pressure CT experiments of *Hashida et al.* [1993]. In both cases loading corresponds to approximately 200 μm of displacement at the gauge (Figure 5). Each box has coordinates corresponding to those of the boundary element mesh (see Figure 4). All stresses are normalized by the peak tensile strength (7 MPa). The tension-softening relation used is the linear approximation (Figure 3, dashed line). Bold lines mark the extent of the process zone, and dashed lines denote the symmetry axis (see Figure 4).

line. Since this additional damage resulted in only a small (several megapascals) increase in the computed breakdown pressure, which lies within the experimental scatter, we conclude that this effect cannot account for the inferred increase in fracture energy, and that the damage around the inner hole does not cause a significant stress relaxation in the vicinity of the "main" crack tip process zone.

Y.M. Khazan (personal communication, 1995) has suggested that some increase in the inferred values of the fracture energy in the high confining pressure experiments of *Abou-Sayed* [1977] could be attributed to the discrete structure of the material, that is, to violation of the postulate of a continuous medium on the scale of the process zone. Estimates of the magnitude of this effect made using analytical solutions for a two-dimensional DB crack in an infinite elastic body, and numerical models designed to mimic the effect of discrete grains, are presented in Appendix B. The estimates obtained are at least a factor of 2 smaller than the deduced increase in the fracture energy, even when the assumed grain size corresponds to largest grains encountered in Indiana limestone. Therefore it does not appear that the difference in fracture energies between the zero and high confining pressure tests results from the dimensions of discrete grains alone.

Although the experimental data of *Abou-Sayed* [1977] do not allow us to determine the variation of each of σ_T and δ_c with confining pressure, the results of direct-pull and four-point beam tensile failure tests performed under ambient compression for several rock types (including Indiana limestone) suggest that the tensile strength σ_T is nearly unaffected by confining pressure [*Brace*, 1964; *Weinberger et*

al., 1994]. Therefore we conclude that the inferred increase in fracture energy may be caused by an increase in the effective critical opening displacement δ_c. Physically, such an increase may result from enhanced inelastic strain (e.g., more extensive distributed microcracking) off of the crack plane, potentially due to the highly anisotropic stress state in the vicinity of the crack process zone (Figure 8).

It is of interest to compare the near-tip stress field in the Abou-Sayed experiments with the near-tip stress field in the CT tests of *Hashida et al.* [1993], in which an increase in fracture energy at high confining pressure was also inferred (see Figure 5). The principal stresses in the vicinity of the process zone for the zero and 26.5 MPa confining pressure experiments are shown in Figure 9 for displacements Δ of about 200 μm. Surprisingly, the size of the region subjected to tension near the tensile strength is larger in the high confining pressure experiments than in the zero pressure tests. This apparently results from the very large crack-parallel extension caused by the enhanced bending of the CT sample under high confining pressure and seems to be a specific feature of the CT configuration. High confining pressure reduces the crack length for a given gauge displacement (Figure 9), and hence results in greater curvature of the beam between the point of force application and the crack tip. The magnitude of this crack-parallel tension (almost 3 times the peak tensile strength, see Figure 9c) poses the question why the crack did not change its direction of propagation by 90° as sometimes happens even in zero pressure tests. Factors that might have stabilized the crack in its own plane are strength anisotropy (the fracture was propagating along the dominant rift plane), and the 3-4 mm deep, 4.3 mm wide grooves cut into the specimen sides to ensure that crack growth remained in the median plane [*Hashida et al.*, 1993]. In either case, it is apparent that the inferred increase in fracture energy in the high confining pressure CT tests could have resulted from enhanced tensile cracking in a larger region (relative to the zero pressure case) off of the crack plane. Thus, even though simulations of both the Abou-Sayed TWC tests and the Hashida et al. CT tests suggest an increase in the effective critical crack opening displacement and fracture energy by a factor of 2 to 3, the causes of the inferred increase appear to be essentially different in the two cases.

As was mentioned above, the TWC experiments of Hashida et al. suggest a decrease in the fracture energy for Iidate granite at confining pressures of 6-8 MPa (Figure 7). The low breakdown pressure may reflect some bias due to the small specimen size. This seems quite plausible, given that the cylinder wall was only 15 mm (about 10 grains) across, and that (using zero-pressure fracture parameters) the computed length of the unbroken ligament at the load corresponding to the observed breakdown pressure would cross only about 4 grains.

Alternatively, a decrease in fracture energy with increasing confining pressure could be physically related to a reduction of the region of absolute tension surrounding the crack tip. It is well known that the fracture energies of rocks are orders of magnitude larger than those of their constituent minerals, although one might expect that the tensile strength of rocks to be generally less than those of their constituent minerals due to the presence of numerous microdefects. The reason for this observation is that "diffuse" microcracking in a three-dimensional (nonplanar) process zone within rocks leads to a significant increase of the total fracture surface, and, ultimately, of the fracture energy [*Friedman et al.*, 1972]. In terms of the idealized DB model, rocks have much higher fracture energies than single crystals because they have much larger values of δ_c, even if they have smaller values of σ_T. Since increased compressive stresses in the vicinity of the process zone may suppress the development and growth of tensile microcracks off of the crack plane, the effective critical opening displacement at high ambient compression may decrease sufficiently to reduce the fracture energy, even if microcrack closure somewhat increases the local tensile strength.

Our simulations show that given a fivefold decrease in δ_c, which satisfies the observed breakdown pressures in the high confining pressure TWC tests of *Hashida et al.* [1993], a phase of stable crack growth exists during which δ_c is reached at the base of the process zone before the sample bursts. Such stable crack growth could be verified experimentally in principle, by monitoring the amount of the injected pressurizing fluid or by measuring the specimen compliance in a fashion similar to the CT experiment. Since in small specimens the load corresponding to the initiation of a stable crack depends critically on the ratio σ_T/δ_c, such data would provide information concerning the individual variations of σ_T and δ_c at high confining pressure. Unfortunately, no corresponding data are available from the *Hashida et al.* [1993] TWC experiments. Thus we cannot distinguish between an actual decrease in the critical opening displacement and a systematic bias in the observed breakdown pressures due to small specimen size. If the low breakdown pressures reflect true reductions in rock fracture energy, we would have to appeal to differences in the near-tip stress field to explain the differences between the two series of high-pressure granite tests.

A systematic dependence of fracture energy on confining pressure and applied loads could have important implications for a number of geological and geotechnical processes involving tensile fracture at depth. However, in order to retard tensile crack growth to an extent that significantly exceeds the direct effect due to the confining pressure alone, the fracture energy would have to increase more dramatically than found in this study. A vivid demonstration of this is the general similarity of the computed load-displacement curves, generated by using different fracture parameters, for the high-pressure CT test of *Hashida et al.* [1993] (Figure 5). One mechanism that could plausibly produce fracture energy increases sufficient to affect the growth of hydrofractures would be some form of scale dependence. A crack tip process zone that scaled with the size of the crack or an unwetted zone near the crack tip would satisfy this criterion. While it is unlikely that process zones tens of centimeters or meters across could be generated in the laboratory, carefully designed experiments might be useful for predictions of process zone size.

Conclusions

Our boundary element simulation of the *Abou-Sayed* [1977] thick-walled cylinder experiments reveal a significant increase in fracture energy (100 to 250%) for Indiana limestone when the confining pressure is raised from 0 to 6 ~ 7 MPa. Based upon analysis of the stress field within the specimen, we suggest that this increase could have been caused by enhanced inelastic deformation off of the crack plane due to large

deviatoric stresses in the vicinity of the process zone. This deformation could generate larger inelastic displacements across the process zone. In terms of the simplified Dugdale-Barenblatt model this would lead to an effective increase in the critical crack wall separation. Data from the compact tension experiments of *Hashida et al.* [1993] at 26 MPa also indicate an increase in the critical opening displacement of a factor of 2 or more, relative to zero pressure experiments. In this case we find that the region of tensile stresses surrounding the process zone was larger in the high-pressure experiments than at zero pressure and suggest that the increase in effective critical crack wall separation may have resulted from an enlarged region of tensile microcracking. These results illustrate the fact that at the same "confining pressure" different loading configurations may affect the process zone in very different ways. While the thick-walled cylinder experiments of *Hashida et al.* [1993] seem to show a decrease in fracture energy with pressure rather than an increase, these results could have been biased because of the very small specimens used.

Our results demonstrate that numerical modeling based on the Dugdale-Barenblatt approach can be extremely useful in designing and interpreting future experiments. For example, such modeling can be used to determine if a particular experimental configuration is sensitive to variations in the cohesive stress or critical crack wall separation, or if the tensile strength of the sample is exceeded anywhere away from the crack tip (e.g., around the inner diameter of the TWC tests of *Abou-Sayed* [1977] or at the step thickness change in the *Hashida et al.* [1993] CT tests). It can also be used to compare the stress field surrounding the process zone in different experimental configurations to an anticipated (computed) near-tip stress field of interest (for example, for a hydrofracture in a region of known ambient differential stress). Because at high confining pressures the near-tip stress field for stably propagating cracks is not a material property, such comparisons are necessary if the results of laboratory tests are to be extrapolated to in situ conditions.

Appendix A

Here we use analytical solutions for a static fluid-filled crack in an infinite elastic solid subjected to a remote compressive stress [*Khazan and Fialko*, 1995] to estimate the process zone length for equilibrium cracks under loading conditions similar to those used in the TWC experiments of *Hashida et al.* [1993]. Consider a two-dimensional crack having a half-length $a = b + \Delta_S + \Delta_T$, where b is the half-length of a fluid-occupied region, Δ_S is the unwetted section length, and Δ_T is the process zone length (Figure B1 of Appendix B). We assume that both the internal fluid pressure P_i (acting on the interval b) and the cohesive stresses σ_T (acting within the process zone Δ_T) are constant and greatly exceed the internal pressure in the unwetted region. Then the following equations must be satisfied for the crack to be on the verge of propagation:

$$\sigma_T = \text{const} = \frac{(P_i - P_c)\arcsin S - P_c \arccos S}{\arccos T}, \tag{A1}$$

$$\delta_c = \frac{2(1-\nu)}{\pi\mu} a \left[P_i\, I(T,S) + 2\,\sigma_T\, T \ln\frac{1}{T} \right], \tag{A2}$$

where μ is the elastic shear modulus, ν is Poisson's ratio, P_i is internal fluid pressure, P_c is confining pressure, $S = 1-(\Delta_T + \Delta_S)/a$, $T = 1-\Delta_T/a$ and the function I is given by [see *Khazan and Fialko*, 1995, equations (9), (13) and (14)]

$$I(U,V) = (V+U)\ln\left|\frac{\sqrt{(1-U^2)(1-V^2)}+1+UV}{V+U}\right| + (V-U)\ln\left|\frac{\sqrt{(1-U^2)(1-V^2)}+1-UV}{V-U}\right| \tag{A3}$$

In the high-pressure TWC tests of *Hashida et al.* [1993], Δ_S=0 (no unwetted zone is present), so $S = T$ and (A1) and (A2) give rise to

$$\delta_c = \frac{4}{\pi}\frac{1-\nu}{\mu} a (\sigma_T + P_i) T \ln\frac{1}{T}. \tag{A4}$$

Noting that $T = b/(b+\Delta_T)$, from (A4) we obtain the following formula for the equilibrium process zone length:

$$\Delta_T = b\left(\exp\left(\frac{\pi}{4}\frac{\mu}{(1-\nu)(\sigma_T + P_i)}\frac{\delta_c}{b} \right) - 1 \right). \tag{A5}$$

For Iidate granite, μ ~ 25 GPa [*Hashida et al.*, 1993], σ_T ~ 6 MPa, and δ_c ~ 0.03 mm (Figure 3). At the confining pressure of 6 MPa the maximum internal pressure P_i in the TWC experiments of Hashida et al. is about 25-30 MPa (Figure 7), and the internal radius of the thick-walled cylinder is b = 6.4 mm. Substituting these values into (A5), we find that a two-dimensional (2-D) crack with similar loading configuration would have a process zone length of the order of 100 mm, which is much larger than the actual thickness of the specimen wall (17-18 mm).

Appendix B

Here we investigate possible effects of the discrete structure of Indiana limestone on the calculated breakdown pressure in the TWC experiments of *Abou-Sayed* [1977]. Our numerical calculations have shown that for realistic values of the tensile strength of Indiana limestone (4-6 MPa) the unwetted region (notch plus the traction-free crack) might comprise a sizable portion of the total crack length in the high confining pressure tests. The corresponding loading configuration for a 2-D crack in an infinite body is shown in Figure B1. In the limit of a large unwetted zone, $\Delta_S \to a$ ($S \to 0$, $T \to 1$), the expressions (A1) and (A2) of Appendix A reduce to

$$\sigma_T = \left(\frac{a}{2\Delta_T}\right)^{1/2}\left(\frac{b}{a}P_i - \frac{\pi}{2}P_c\right), \tag{B1}$$

$$\delta_c = \frac{2(1-\nu)}{\pi\mu} a \left[\frac{2b}{a}\left(\frac{2\Delta_T}{a}\right)^{1/2} P_i + \frac{2\Delta_T}{a}\sigma_T \right]. \tag{B2}$$

In the high-pressure TWC tests of Abou-Sayed, b = 4.75 mm, a = 25~30 mm (Figure 8), P_i ~ 50 MPa and σ_T ~ 5 MPa. We

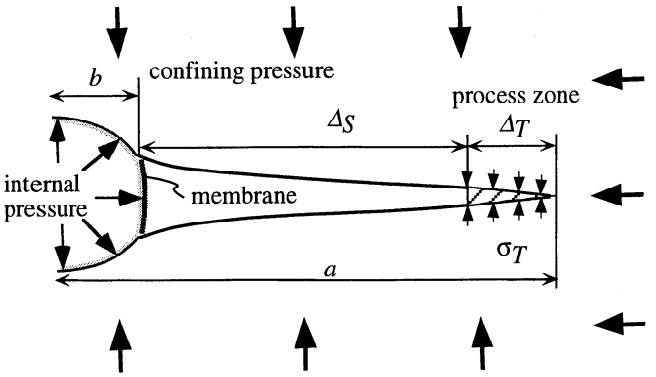

Figure B1. Schematic view of a two-dimensional DB crack in the approximation of a large unwetted zone. An impermeable membrane, placed at a distance b from the crack center, does not allow the pressurizing fluid to advance and penetrate the rest of the crack. As the internal fluid pressure in the wetted region is increased, the process zone will move forward leaving the empty (traction-free) crack behind. Cohesive tractions σ_T act within the process zone having length Δ_T; Δ_S is the unwetted zone length. Note that both in the *Abou-Sayed* [1977] and *Hashida et al.* [1993] experiments the internal holes of cylindrical samples were lined in order to prevent the pressurizing medium from reaching the crack surfaces and infiltrating the specimen.

note that the second term in brackets on the right-hand side of (B2) is small compared to the first term (even if the ratio $2\Delta_T/a$ is not negligibly small) and may be omitted. Then the expression for the fracture energy G_c can be written as

$$G_c = \sigma_T \delta_c = \frac{4(1-\nu)}{\pi\mu} b n P_c^2 \left(n\frac{b}{a} - \frac{\pi}{2}\right), \qquad \text{(B3)}$$

where $n = P_i/P_c$.

If the crack tip propagates stepwise such that the minimum possible crack length increment is Δa (which may physically correspond to the dimension of the grains or other structural irregularities), the corresponding variation of fracture energy will be of the order of

$$\Delta G_c = -\frac{4(1-\nu)}{\pi\mu}\left(\frac{bnP_c}{a}\right)^2 \Delta a + O(\Delta a^2). \qquad \text{(B4)}$$

Although the model shown in Figure B1 is not directly analogous to the TWC configuration because the boundary conditions are not identical and the process zone in the *Abou-Sayed* [1977] high-pressure tests may not be small compared to the total crack length, we expect that (B4) captures many of the essential effects of discrete changes in fracture length in the high-pressure TWC tests. Substituting values from the *Abou-Sayed* [1977] configuration ($n = 8$, P_c = 6 ~ 7 MPa, $\Delta a = 0.5 \sim 2$ mm (grain size) [*Ingraffea and Schmidt*, 1978], μ = 13 GPa, $\nu = 0.25$), ΔG_c is estimated to be 2 ~ 15 J m^{-2}. This result demonstrates that small fluctuations of the actual crack length may give rise to large variations of the experimentally deduced fracture energy. Note, however, that in order to explain the consistent increase of fracture energy, the actual crack must be consistently shorter than predicted by the plane strain solution everywhere along the crack front (i.e., $\Delta G_c > 0$ when $\Delta a < 0$ in (B4)). This seems unlikely because in a three-dimensional granular material it is reasonable to expect the crack to be both longer and shorter along the crack front than predicted by the continuum 2-D model. A full analysis of the effect of rock microstructure in this case should account for the deviation of the crack front from a straight line [e.g., *Rice*, 1985].

Additional numerical tests were performed for the high-pressure TWC experiments of *Abou-Sayed* [1977] in which (1) various coarse grids, intended to mimic discrete grains, were used in the vicinity of the crack tip, and (2) strength inhomogeneities were introduced along the process zone to mimic the alternation of "strong" (σ_T =6 MPa) and "weak" (σ_T =0 MPa) grains in such a way that the average fracture energy is unchanged. As is shown in Figure B2, for "grains" larger than 1 mm there is an increase in the observed breakdown pressure, and this effect is more pronounced for the "inhomogeneous" process zone. At zero pressure this effect is not observed because the process zone comprises a major part of the total crack length and each "grain" represents only a small fraction of the process zone length. For the heterogeneous process zone, increasing the boundary element size from 0.5 to 2-3 mm corresponds to increases in the breakdown pressure of 4-6 MPa, which translates into a 10 to 15 J m^{-2} increase in the "apparent" fracture energy (see Figure 2). These numbers are close to those obtained using the analytical solution above. Therefore we conclude that even though the discrete structure of the material could be responsible for a significant fraction of the increase in the fracture energy deduced for Indiana limestone, the magnitude of this effect would be at least a factor of 2 smaller than the increase inferred from our simulations of the TWC experiments of *Abou-Sayed* [1977], even in the unlikely case that the crack front was arrested at the last stable configuration by a line of statistically large, strong grains. For the average grain size of 1 mm, this effect could account for only 10-20% of the inferred increase of the fracture energy of Indiana limestone.

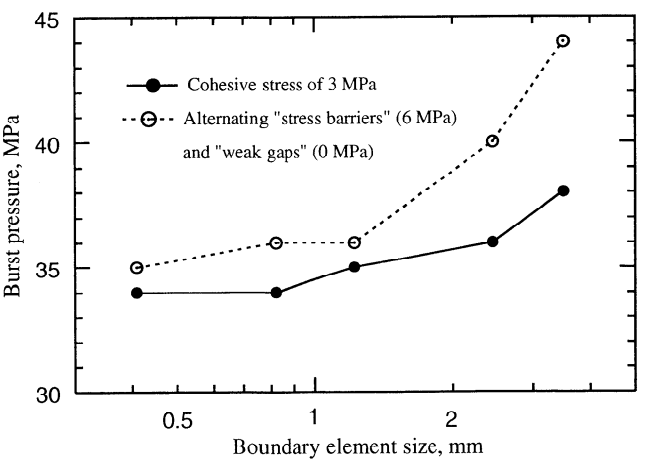

Figure B2. Variation in the calculated breakdown pressures for the high-pressure TWC tests of *Abou-Sayed* [1977] as a function of the mesh discretization along the prospective crack growth line. Dashed line corresponds to a model of a process zone having "inhomogeneous" strength distribution, in which the "strong" boundary elements were alternated with the elements having zero strength along the process zone. In both simulations fracture energy equals 30 J m^{-2} and increments in the internal fluid pressure equal 1 MPa.

Acknowledgments. We thank Leonid Germanovich, Andreas Kronenberg, and an anonymous referee for useful reviews that helped to clarify the early version of this manuscript.

References

Abou-Sayed, A.S., Fracture toughness, K_{1C}, of triaxially-loaded Indiana limestone, *Proc. U.S. Rock Mech. Symp., 18th,* 2A3/1-2A3/8, 1977.

Atkinson, B.K., and P.G. Meredith, Experimental fracture mechanics data for rocks and minerals, in *Fracture Mechanics of Rock,* edited by B.K. Atkinson, pp. 477-525, Academic, San Diego, Calif., 1987.

Barenblatt, G.I., The mathematical theory of equilibrium cracks in brittle fracture, *Adv. Appl. Mech., 7,* 55-129, 1962.

Brace, W.F., Brittle fracture of rocks, in *State of Stress in the Earth's Crust,* edited by W.R. Judd, pp. 111-178, Elsevier, New York, 1964.

Brebbia, C.A., and J. Dominguez, *Boundary Elements: An Introductory Course,* 331 pp., McGraw-Hill, New York, 1991.

Cleary, M.P., C.A. Wright, and T.B. Wright, Experimental and modeling evidence for major changes in hydraulic fracturing design and field procedures, paper presented at SPE Gas Technology Symposium, Soc. of Pet. Eng., Houston, Texas, Jan. 23-25, 1991.

Crouch, S.L., and S.M. Starfield, *Boundary Element Methods in Solid Mechanics: With Applications in Rock Mechanics and Geological Engineering,* 322 pp., Allen and Unwin, Winchester, Mass., 1983.

Delaney, P.T., D.D. Pollard, J.I. Ziony, and E.H. McKee, Field relations between dikes and joints: Emplacement processes and paleostress analysis, *J. Geophys. Res., 91,* 4920-4938, 1986.

Dyskin, A.V., and L.N. Germanovich, A model of crack growth in microcracked rock, *Int. J. Rock Mech. Min. Sci. Geomech. Abstr., 30,* 813-820, 1993.

Friedman, M., J. Handin, and G. Alani, Fracture-surface energy of rocks, *Int. J. Rock Mech. Min. Sci., 9,* 757-766, 1972.

Hashida, T., H. Oghikubo, H. Takahashi, and T. Shoji, Numerical simulation with experimental verification of the fracture behavior in granite under confining pressures based on the tension-softening model, *Int. J. Fract., 59,* 227-244, 1993.

Ingraffea, A.R., Theory of crack initiation and propagation in rock, in *Fracture Mechanics of Rock,* edited by B.K. Atkinson, pp. 277-349, Academic, San Diego, Calif., 1987.

Ingraffea, A.R., and R.A. Schmidt, Experimental verification of a fracture mechanics model for tensile stress prediction of Indiana limestone, *Proc. U.S. Rock Mech. Symp., 19th,* 247-253, 1978.

Khazan, Y.M., and Y.A. Fialko, Fracture criteria at the tip of fluid driven cracks in the Earth, *Geophys. Res. Lett., 22,* 2541-2544, 1995.

Labuz, J.F., S.P. Shah, and C.H. Dowding, The fracture process zone in granite: Evidence and effect, *Int. J. Rock Mech. Min. Sci. Geomech. Abstr., 24,* 235-246, 1987.

Lawn, B.R., and T.R. Wilshaw, *Fracture of Brittle Solids,* 204 pp., Cambridge Univ. Press, New York, 1975.

Lister, J.R., and R.C. Kerr, Fluid-mechanical models of crack propagation and their application to magma transport in dykes, *J. Geophys. Res., 96,* 10,049-10,077, 1991.

Lockner, D.A., J.D. Byerlee, V. Kuksenko, A. Ponomarev, and A. Sidorin, Observations of quasi-static fault growth from acoustic emissions, in *Fault Mechanics and Transport Properties of Rocks,* edited by B. Evans and T. Wong, pp. 3-32, Academic, San Diego, Calif., 1992.

Rice, J.R., Mathematical analysis in the mechanics of fracture, in *Fracture: An Advanced Treatise,* edited by H. Liebowitz, pp. 192-314, Academic, San Diego, Calif., 1968.

Rice, J.R., First-order variation in elastic fields due to variation in location of a planar crack front, *J. Appl. Mech., 52,* 571-579, 1985.

Roegiers, J.-C., and X.L. Zhao, Rock fracture tests in simulated downhole conditions, in *Symposium on Rock Mechanics as a Multidisciplinary Science,* edited by J.-C. Roegiers, A. A. Balkema, Brookfield, Vermont., pp. 221-231, 1991.

Rubin, A.M., Tensile fracture of rock at high confining pressure: Implications for dike propagation, *J. Geophys. Res., 98,* 15,919-15,935, 1993.

Schmidt, R.A., Fracture-toughness testing of limestone, *Exp. Mech., 16,* 161-176, 1976.

Schmidt, R.A., and C.W. Huddle, Effect of confining pressure on fracture toughness of Indiana limestone, *Int. J. Rock Mech. Min. Sci. Geomech. Abstr., 14,* 289-293, 1977.

Shlyapobersky, J., and A. Chundovsky, Fracture mechanics in hydraulic fracturing, *Proc. U.S. Rock Mech. Symp., 33rd,* 827-836, 1992.

Spence, D.A., and D.L. Turcotte, Magma-driven propagation of cracks, *J. Geophys. Res., 90,* 575-580, 1985.

Stevenson, D.J., Migration of fluid-filled cracks: Applications to terrestrial and icy bodies, *Proc. Lunar Planet. Sci. Conf., 13th,* Part 1, *J. Geophys. Res., 87,* suppl., A1-A480, 1982.

Swanson, P.L., Tensile fracture resistance mechanisms in brittle polycrystals: An ultrasonic and in situ microscopy investigation, *J. Geophys. Res., 92,* 8015-8036, 1987.

Thiercelin, M., Fracture toughness under confining pressure using the modified ring test, *Proc. U.S. Rock Mech. Symp., 28th,* 149-156, 1987.

Weinberger, R., Z. Reches, T. Scott, and A. Eidelman, Tensile properties of rocks in four-point beam tests under confining pressure, in *Rock Mechanics Models and Measurements: Challenges from Industry,* edited by P.P. Nelson, A. A. Balkema, Brookfield, Vermont., pp. 435-442, 1994.

Y. A. Fialko and A. M. Rubin, Department of Geosciences, Princeton University, Princeton, NJ 08544 (e-mail: fialko@geo.princeton.edu; allan@geo.princeton.edu).

(Received February 12, 1996; revised December 2, 1996; accepted December 9, 1996.)